

## EPR Study of the Low-Spin $[d^3; S = 1/2]$ , Jahn–Teller-Active, Dinitrogen Complex of a Molybdenum Trisamidoamine

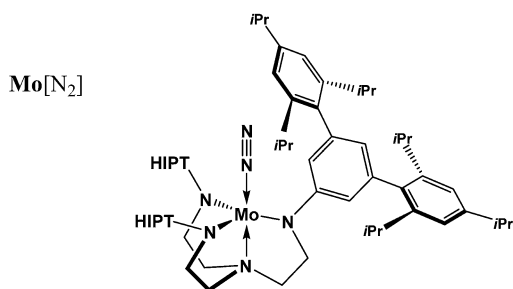
Rebecca L. McNaughton,<sup>†</sup> Jia Min Chin,<sup>‡</sup> Walter W. Weare,<sup>‡</sup> Richard R. Schrock,<sup>\*,‡</sup> and Brian M. Hoffman<sup>\*,†</sup>

Department of Chemistry, Northwestern University, 2145 Sheridan Road, Evanston, Illinois 60208-3113, and Department of Chemistry, Massachusetts Institute of Technology, Cambridge, Massachusetts 02139

Received November 28, 2006; E-mail: bmh@northwestern.edu; rrs@mit.edu

The sterically encumbered trisamidoamine (TAA) complex<sup>1,2</sup>  $[\text{Mo}] = \text{Mo}[\text{HIPTN}_3\text{N}]$ , Inset 1, is extremely important for its ability to catalyze the reduction of  $\text{N}_2$  to  $\text{NH}_3$ ,<sup>3</sup> and for the mechanistic insights into this process that it provides; of the thirteen compounds that are postulated to be involved in the formation of  $2\text{NH}_3$ , the structures of eight already have been determined by X-ray diffraction.<sup>4,5</sup> Nonetheless, at present there is little understanding of the particular features of the electronic structure of the  $[\text{Mo}]L$  complexes that underlie their reactivity.

### Inset 1

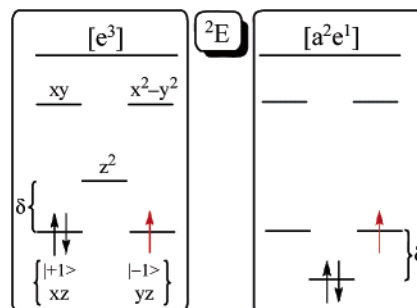


The key first step in the catalytic cycle is  $\text{N}_2$ -bound  $[\text{Mo}]\text{N}_2$ ,<sup>6</sup> (Inset 1) which contains a Mo(III) that has been shown by magnetic susceptibility measurements to have a low-spin (ls)  $[d^3; S = 1/2]$  electronic configuration. It has not been emphasized that this is one of the rarest configurations in coordination chemistry. To our knowledge, there is only one report of a ls- $[d^3]$  complex of any transition ion prior to the synthesis of the TAA complexes.<sup>7</sup> Nor has it been noted that a ls- $[d^3]$  ion in the trigonal-bipyramidal coordination environment of  $[\text{Mo}]\text{N}_2$  exhibits a doubly degenerate  ${}^2E$  ground state, Scheme 1, that is subject to a Jahn–Teller (JT) distortion by vibronic coupling to doubly degenerate  $e_2$  vibrations.<sup>8,9</sup> Indeed, as shown in the scheme, this ls- $[d^3]$  complex has two possible electronic configurations:  $[e^3]$  and  $[a^2e^1]$ , each doubly degenerate. Although the former is suggested to apply,<sup>4</sup> this has not been tested. This report first describes the possible vibronic behaviors of  $[\text{Mo}]\text{N}_2$ . It then presents an EPR study that characterizes the electronic configuration and vibronic properties of this complex.

Both  $[d^3; S = 1/2]$  configurations of Scheme 1 exhibit unquenched orbital angular momentum, and splitting of the orbital degeneracy by spin–orbit coupling (SOC) competes with the JT effect (JTE). Linear vibronic coupling is describable in terms of a single composite (“interaction”)  $e_2$  mode,<sup>8</sup> in which the molecule undergoes a “pseudo-Jahn–Teller” (PJT) distortion,  $\rho_0$ ,<sup>8</sup>

$$\rho_0 = [(F/K)^2 - (\lambda/2F)^2]^{1/2} \quad (1)$$

### Scheme 1



provided the JT vibronic coupling is strong enough, namely  $\rho_0$  is real. Here  $K$  is the effective force constant of the interaction mode,  $F$  is the linear coefficient of vibronic coupling to this mode, and  $\lambda$  is the SOC constant. This PJT effect replaces the electronic degeneracy with a vibronic degeneracy in which the complex is distorted (e.g., equilateral  $\rightarrow$  isosceles triangle; axial  $\rightarrow$  nonaxial  $\text{N}_2$ ) and the distortion “pseudorotates”. If the JT vibronic coupling is weak ( $\rho_0$  is imaginary) the JT distortion is quenched and  $[\text{Mo}]\text{N}_2$  retains the trigonal symmetry.

The molecular adiabatic potential energy surface (APES) of an isolated molecule is a function of the PJT distortion,  $\rho$ , but is independent of the phase angle ( $\phi$ ) that defines the direction of the distortion. One must further allow for a solvent-dependent environmental contribution to the  $e$ -orbital splitting, the “solvent potential”,  $V_L$ ,<sup>10</sup> resulting in APES energies,  $W_{\pm} = K\rho^2/2 \pm 2[(\lambda/2)^2 + (F\rho \sin \phi)^2 + (F\rho \cos \phi + V_L)^2]^{1/2}$ . When  $V_L = 0$ , the ground APES ( $W_-$ ) is the well-known “modified Mexican hat” (Figure 1A) with the minimum of the “trough” at  $\rho_0$ .<sup>8,9</sup>  $V_L \neq 0$  skews the ground APES, (Figure 1B) favoring a particular distortion. At low temperatures, the dynamic PJT distortion will localize at the skewed APES minimum; localization also is favored by quadratic JT coupling.<sup>8</sup>

The X-band CW EPR spectrum of  $S = 1/2$   $[\text{Mo}]\text{N}_2$  in toluene, Figure 2,<sup>11,12</sup> exhibits axial symmetry with  $g_{\perp} = 1.61 < 2 < g_{\parallel} = 3.03$ ; identical values were obtained from Q-band CW and spin echo-EPR spectra. The  $g$ -values distinguish unambiguously between the  $[e^3]$  and  $[a^2e^1]$  configurations, and give insights into the vibronic

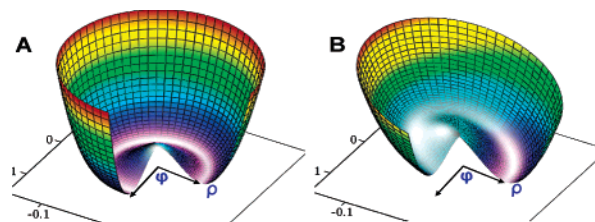
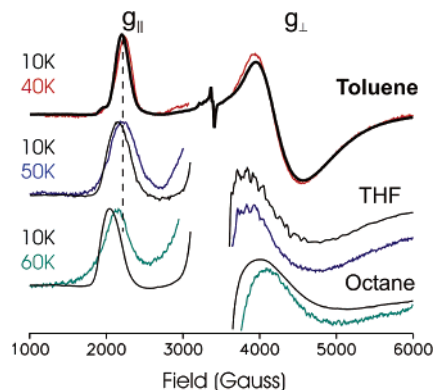


Figure 1. Lower PJT APES ( $W_-$ ) calculated with (A)  $\lambda = 800 \text{ cm}^{-1}$ ,  $K = 1 \text{ mdyne/A}$ ,  $F\rho_0 = 0.95\lambda$ ; (B) as in panel A, but with  $V_L = 0.1\lambda$ .

<sup>†</sup> Northwestern University.

<sup>‡</sup> Massachusetts Institute of Technology.



**Figure 2.** 9.36 GHz EPR of  $[\text{Mo}]\text{N}_2$ . The “gaps” at  $g \approx 2$  in some spectra eliminate signals from decomposition products and/or precipitated complex in the poorly glassing THF and octane, chosen to vary  $V_L$ .

and solvent interactions. We consider a two-orbital model Hamiltonian in which vibronic coupling with the interaction mode combines with SOC to mix and split the  $e(xz, yz; m_S = \pm 1)$  orbitals.<sup>13</sup> This PJT model gives an axial  $g$ -tensor for the ground APES with  $g_{||}$  along the trigonal axis. The  $[g_{||}, g_{\perp}]$  components at the APES minimum depend on the ratio of the sum of equilibrium distortion and environmental energies to the SOC,  $[(F\rho_0) + V_L/2]/\lambda$ , through the fictitious angle  $2\theta$ :

$$\tan 2\theta = 2[F\rho_0 + V_L/2]/\lambda \quad (2)$$

$$[e^3] g_{||} = 2(1 + k \cos 2\theta) \quad (3a)$$

$$[a^2e^1] g_{||} = 2(1 - k \cos 2\theta) \quad (3b)$$

$$g_{\perp} = (2 \sin 2\theta) \quad (3c)$$

The quantity  $(1 - k)$  corresponds to d-electron delocalization. As  $2\theta$  increases from 0 (JTE quenched; no distortion) to  $\pi/2$  (SOC quenched), the  $[e^3]$  configuration gives  $[0 \leq g_{\perp} \leq 2; 4 \geq g_{||} \geq 2]$ , while  $[a^2e^1]$  gives  $[0 \leq g_{||} \leq g_{\perp} \leq 2]$ . The observed  $g$ -values thus require the  $[e^3]$  configuration for  $[\text{Mo}]\text{N}_2$ . Analysis further gives d-electron delocalization of  $(1 - k) = 15\%$  and a distortion energy with  $\tan 2\theta = 1.4$ . The PJT splitting between the lower APES minimum and the upper APES is large,  $\Delta E(\rho_0) = 2\lambda[(1/2)^2 + ((\tan 2\theta)/2)^2]^{1/2} \approx 2\lambda \approx 1600 \text{ cm}^{-1}$ .<sup>14</sup> As a result, the ground and excited APES should be vibronically decoupled (“strong-coupling” or adiabatic limit), and the system well-described by the ground APES and its  $g$ -values.<sup>8,9</sup> The JT energies may even be large enough to have an influence on the energetics of  $\text{N}_2$  reduction.

Variations in the  $g$ -values with solvent,  $g_{||} = 3.03$  (toluene), 3.10 (THF), 3.26 (octane) (Figure 2) reveal an environmental influence.<sup>10</sup> Taking octane as approximating a nonperturbing environment,  $V_L(\text{octane}) \approx 0$ , the  $g$ -values provide interaction parameters through eq 2:  $F\rho_0/\lambda \approx 1$ ,  $V_L(\text{THF})/\lambda \approx 0.3$ , and  $V_L(\text{toluene})/\lambda \approx 0.4$ . The small environmental term,  $F\rho_0 > V_L$ , contrasts with the PJT-active  $\text{MCP}_2$ ,<sup>10,16</sup>  $\text{M} = \text{Co(II)}$ ,  $\text{Fe(I)}$ , and  $\text{Fe(III)}$ , where  $F\rho_0 \ll V_L$ .<sup>10,15–17</sup> The reversal of this inequality for  $[\text{Mo}]\text{N}_2$  is noteworthy, as the bulky HIPT substituents were in fact incorporated to shield the metal center from its environment.

The  $g$ -values of  $[\text{Mo}]\text{N}_2$  in toluene do not shift significantly as temperature increases, whereas in THF and octane, solvents with smaller  $V_L$ , the  $g$ -values shift slightly (Figure 2). Unlike the well-studied JTE for  $\text{Cu(II)}$ ,<sup>8,9,17</sup> this behavior cannot be used as evidence regarding possible reorientation of a trapped JT distortion. Warping of the ground APES of  $\text{Cu(II)}$  ions leads to three alternate JT distortion orientations with different  $g$ -tensor orientations, and thermally activated reorientation of the distortion can cause strong

“motional” effects in the  $\text{Cu(II)}$   $g$ -values. In contrast,  $g_{||}$  for  $[\text{Mo}]\text{N}_2$  is oriented along the trigonal axis for all orientations of the PJT distortion (angles,  $\phi$ ), so reorientation has no effect. We instead attribute  $g$ -shifts to thermal excitations within the energy “well” of the skewed APES (Figure 1B), which is shallower for smaller values of  $V_L$ . The EPR signal for  $[\text{Mo}]\text{N}_2$  in toluene does not broaden with increasing temperature; those for  $[\text{Mo}]\text{N}_2$  in THF and octane broaden only slightly (Figure 2). This contrasts with the substantial broadening from Orbach relaxation by low-lying states of the PJT-active  $\text{MCP}_2$ ,<sup>10,15</sup> and indicates that  $[\text{Mo}]\text{N}_2$  has no low-lying excitations ( $\delta$ , Scheme 1, is large).<sup>18</sup>

In summary, this first EPR study of an  $[\text{Mo}]\text{L}$  complex establishes that  $[\text{Mo}]\text{N}_2$  exhibits the  $1s[e^3]$  electronic configuration and the JTE in the vibronic strong-coupling (adiabatic) limit. The antibonding  $a(z^2)$  orbital is considerably higher in energy than  $e(xz, yz)$ , presumably because of interactions with the axial nitrogen atoms. It appears that interactions with the solvent localize the PJT distortion of  $[\text{Mo}]\text{N}_2$  at low temperatures, even though the complex is highly sterically encumbered. If there is no PJT distortion or a pseudorotating one, hyperfine tensors of the in-plane N atoms as determined by <sup>14,15</sup>N ENDOR studies of  $[\text{Mo}]\text{N}_2$  (in progress) will be identical; if skewing of the APES selects a particular distortion, as proposed, they will not be equal. DFT computations are in progress to identify the vibrations that contribute to the composite interaction mode. ENDOR studies of  $[\text{Mo}]\text{N}_2$  and other  $[\text{Mo}]\text{L}$  also will permit comparison with intermediates trapped during the turnover of nitrogenase.<sup>19,20</sup>

**Acknowledgment.** This work was supported by the NIH (HL13531, B.M.H.; GM31978, R.R.S.; GM067349, R.L.M.) and NSF (MCB0316038, B.M.H.). We thank Prof. J. Telsler for insightful remarks and Mr. Clark Davoust for technical assistance.

## References

- (1) HIPT = hexaisopropylterphenyl;  $[\text{HIPTN}_3\text{N}]^{3-} = [3,5-(2,4,6\text{-}i\text{-Pr}_3\text{-C}_6\text{H}_2)_2\text{C}_6\text{H}_3\text{NCH}_2\text{CH}_2]_3\text{N}^{3-}$
- (2) Laplaza, C. E.; Cummins, C. C. *Science* **1995**, *268*, 861–863.
- (3) Yandulov, D. V.; Schrock, R. R. *Science* **2003**, *301*, 76–78.
- (4) Schrock, R. R. *Philos. Trans. R. Soc. London, Ser. A* **2005**, *363*, 959–969.
- (5) (a) Schrock, R. R. *Acc. Chem. Res.* **2005**, *38*, 955. (b) Weare, W. W.; Dai, C.; Byrnes, M. J.; Chin, J.; Schrock, R. R.; Müller, P. *Proc. Nat. Acad. Sci. U.S.A.* **2006**, *103*, 17099–17106.
- (6) (a) Yandulov, D. V.; Schrock, R. R. *Inorg. Chem.* **2005**, *44*, 1103. (b) Weare, W. W.; Schrock, R. R.; Hock, A. S.; Mueller, P. *Inorg. Chem.* **2006**, *45*, 9185–9196.
- (7) Rossman, G. R.; Tsay, F. D.; Gray, H. B. *Inorg. Chem.* **1973**, *12*, 824–829.
- (8) Bersuker, I. B. *The Jahn–Teller Effect*, 1st ed.; Cambridge University Press: Cambridge, U.K., 2006.
- (9) Englman, R. *The Jahn–Teller Effect in Molecules and Crystals*; Monographs in Chemical Physics Series; Wiley-Interscience: London, 1972.
- (10) Ammeter, J. H. *J. Magn. Reson.* **1978**, *30*, 299–325.
- (11) X-band EPR spectra were collected with a Bruker ESP300 spectrometer equipped with an Oxford ITC503 cryostat.
- (12) The <sup>95,97</sup>Mo (23% abundance) hyperfine pattern,  $A_{||} \approx 45\text{--}50 \text{ G}$  is visible as a low-field shoulder on  $g_{||}$  of the toluene spectrum.
- (13) For large  $g$  shifts, as seen here, coupling to the  $[xy, x^2 - y^2]$  orbitals can be ignored.
- (14) Weil, J. A.; Bolton, J. R.; Wertz, J. E. *Electron Paramagnetic Resonance: Elementary Theory and Practical Applications*; John Wiley & Sons, Inc: New York, 1994.
- (15) Ammeter, J. H.; Swalen, J. D. *J. Chem. Phys.* **1972**, *57*, 678–698.
- (16) This potential is equivalent to the strain that influences the JT effect in  $\text{Cu(II)}$  crystals studied by Hitchman and co-workers.
- (17) Hitchman, M. A.; Yablokov, Y. V.; Petrashen, V. E.; Augustyniak-Jablokov, M. A.; Strateimeier, H.; Riley, M. J.; Lukaszewicz, K.; Tomaszewski, P. E.; Pietraszko, A. *Inorg. Chem.* **2002**, *41*, 229–238.
- (18) It will be shown elsewhere that the observation of an axial EPR signal (Figure 2) implies that  $\delta/\lambda > 7\text{--}10$ .
- (19) Dos Santos, P. C.; Igarashi, R. Y.; Lee, H.-I.; Hoffman, B. M.; Seefeldt, L. C.; Dean, D. R. *Acc. Chem. Res.* **2005**, *38*, 208–214.
- (20) Barney, B. M.; Yang, T.-C.; Igarashi, R. Y.; Santos, P. C. D.; Laryukhin, M.; Lee, H.-I.; Hoffman, B. M.; Dean, D. R.; Seefeldt, L. C. *J. Am. Chem. Soc.* **2005**, *127*, 14960–14961.

JA068546U